International Journal of Bio-Science and Bio-Technology
Vol.6, No.3 (2014), pp.97-108
http://dx.doi.org/10.14257/ijbsbt.2014.6.3.12

Multimodal Medical Image Fusion using Neighbouring Pixel Selection

S.Sivasangumani[1], P.S .Gomathi[2] and B. Kalaavathi[3]

[1]IEEE Member , P.G Scholar, Department of Electronics and Communication Engineering, V.S.B. Engineering College, Affiliated to Anna University, Karur, Tamil Nadu, India

[2]Assistant Professor, Department of Electronics and Communication Engineering, V.S.B. Engineering College, Affiliated to Anna University, Karur, Tamil Nadu, India

[3] Professor, Department of Computer Science and Engineering, K.S.R. Institute for Engineering and Technology, Affiliated to Anna University, Tiruchengode, Tamil Nadu, India

sivasangumani@gmail.com, gomsps@gmail.com, kalabhuvanesh@gmail.com

Abstract

Medical data analysis from different medical image sensor has been increased in medical field. The image fusion techniques which are the efficient way of adding and improving medical imaging information have drawn increasing concentration from the medical society. In this paper, we proposed a new scheme of Neighbouring Pixel Selection (NPS) fusion rule for laplacian pyramidal multiscale decomposition-based fusion of medical images considering the consistency verification of both intrascale and interscale parameters. A combining set of coefficients from the Multiscale Representations (MSR) of the source images is computed by utilization of neighborhood information. An efficient fusion scheme is also proposed for different modalities. Experimental results show that proposed method produces better results than the existing methods.

Index Terms: *Image fusion, LPT decomposition, Membership Functions, NPS fusion rule, Medical Image Fusion, Multiscale Analysis*

I. Introduction

For diagnosis and treatment, the multimodal medical imaging is very important because each modality provide different information. However, each imaging modality only provides information in a limited domain, many studies prefer joint analysis of imaging data collected from the same patient using different modalities. This requirement of joint analysis led to the introduction of image fusion into the medical field and the development of medical data-oriented fusion techniques. The goal of image fusion is to provide a single fused image, which provides more accurate and reliable information than any individual source image in which features may be more distinguishable [1]. Such an enhanced image facilitates visual perception or further image processing.

Image fusion can be performed at three different levels, pixel/data level, feature/attribute level, and symbol/decision level, each of which serves different purposes [1-3]. Compared with the others, pixel-level fusion directly combines the original information in the source images and is more computationally efficient [3]. According to whether multiscale decomposition (MSD) is used, pixel-level fusion methods can be classified as MSD-based or non-MSD based. Compared to the latter, MSD-based methods have the advantage of extracting and combining salient features at different scales, and therefore normally produce images with greater information content.

ISSN: 2233-7849 IJBSBT

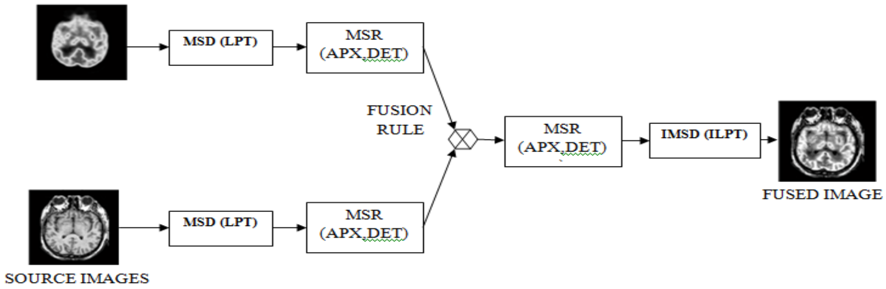

Figure 1. General Procedure of MSD-based Fusion

The general procedure of MSD-based fusion is illustrated in Figure 1. First, the source images are transformed to multiscale representations (MSRs) using MSD. An MSR is a pyramidal structure with successively reduced spatial resolution; it usually contains one approximation level (APX) storing low-pass coefficients and several detail levels (DETs) storing high-pass or band pass coefficients. Then, a certain fusion rule is applied to merge coefficients at different scales. Finally, an inverse MSD (IMSD) is applied to the fused MSR to generate the final image.

Two schemes can be explored in MSD based fusion to enhance the fusion quality; advanced MSD schemes and effective fusion rules. Here, we focus on the latter and propose a novel NPS fusion rule, where the belongingness/membership of each fused coefficient to each source image is calculated. Unlike previous methods, our fusion rule calculates an optimal set of coefficients for each scale taking into account large neighborhood information, which guarantees intrascale and interscale consistencies, *i.e.*, coefficients with similar characteristics are fused in a similar way and artifacts (*e.g.*, aliasing artifacts at object boundaries [4]) are avoided in the results.

II. Fusion Rules

In addition to the MSD scheme, the other key factor affecting fusion results is the fusion rule. A fusion rule is the processing that determines the formation of the fused MSR from the MSRs of the source images, and it normally consists of four key components, *i.e.*, activity-level measurement, coefficient grouping, coefficient combination, and consistency verification [5]. In this section, we give a brief review of some representative schemes in these four steps. Please refer to [5] and [6] for more detailed discussions and other types of fusion methods (*e.g.*, estimation theory-based method [7]).

1. Activity-Level Measurement

The activity-level measurement reflects the salience of each coefficient in MSR and it can be categorized into three classes. 1. Coefficient-based activity (CBA), 2.Window-based activity (WBA), 3. Region-based activity (RBA). A CBA measure evaluates each coefficient independently and normally describes the activity level of a coefficient using its absolute value. A WBA measure uses the information within a window to evaluate the coefficient at the window center. A popular choice is the rank filter-based WBA, where the maximum value within a window is normally selected as in [7]. In our NPS rule, there is no restriction on the type of activity-level measures to be employed. The focus of our NPS rule is to provide a unified framework for the other three key components in a fusion rule, which were usually treated separately in previous methods.

2. Coefficient Grouping

The coefficient grouping schemes can be roughly divided into four categories [1], No grouping (NG), Single-scale grouping (SG), Multiscale grouping (MG), Cross-band SG (CBSG). NG means that each coefficient is fused independently; SG means that corresponding coefficients between different sub-bands at the same scale are fused in the same way; and MG is more restrictive than SG because it also requires that corresponding coefficients between different scales take the same fusion decision. A cross-band SG (CBSG) scheme was proposed in [8], where the same fusion decision for every set of corresponding detail coefficients at the current scale is made based on the sum of their activity levels and their corresponding coefficients at a higher scale. In [9], an MG scheme was proposed in which the fusion decision for every set of corresponding coefficients across all scales is made based on the weighted average of their activity levels. Our NPS rule performs similar to MG, but does not impose such a hard constraint on the fusion decision. Instead, the influence on each coefficient from their corresponding coefficients at adjacent scales is reflected in the membership calculation, and the fusion decision of a coefficient is determined based on its calculated membership.

3. Coefficient Combination

One common coefficient combination scheme for the DETs is the choose-max (CM) strategy, *i.e.*, selecting the coefficient with the highest activity level at each location from the MSRs of the source images as the coefficient at that location in the MSR of the fused image. Three common combination schemes for APX are Choose-Max (CM), Average (AVG) and Weighted average (WA) [10]. In WA, a linear weighting function is applied when the local correlation between corresponding coefficients in a neighborhood in the MSRs of the source images is above a threshold. Our NPS rule does not apply combination schemes based directly on coefficient activity levels, but combines coefficients based on their memberships, which results in a more effective scheme utilizing interscale and intrascale information.

4. Consistency Verification

The consistency verification schemes ensure that neighboring coefficients are fused in a similar manner. A majority filter is used in Window-based verification (WBV), Cross-band verification (CBV), No verification (NV) schemes which was proposed in [7], where the coefficients at a DET are recalculated if their corresponding coefficients at a lower level do not come from the same MSR. CBV was designed to comply with CBSG. It is also possible that no verification (NV) is applied. Our NPS rule does not perform explicit verification, but embeds verification in the coefficient membership calculation process.

III. Neighbouring Pixel Selection (NPS) Method

1. Medical Image Fusion

Here we discuss some activity-level measures and non-MSD based methods proposed for medical image fusion. Please note that the MSD-based fusion methods discussed in the previous sections can be applied directly to medical image fusion; the DWT+CBA+NG+AVG+CM+NV method, for example, was used in [11] for quality enhancement of real-time 3-D echocardiography. A multichannel pulse coupled neural net-work was proposed in [12] for 2-D medical image fusion. However, the fusion results suffered from loss of local contrast. DWT+WBA+NG+CM+CM+WBV was applied to fuse 2-D medical images in [13], where a visibility-based WBA and a local variance-based WBA were proposed for APX and DETs, respectively. In contrast, our focus here is a novel fusion rule rather than a specific activity-level measure.

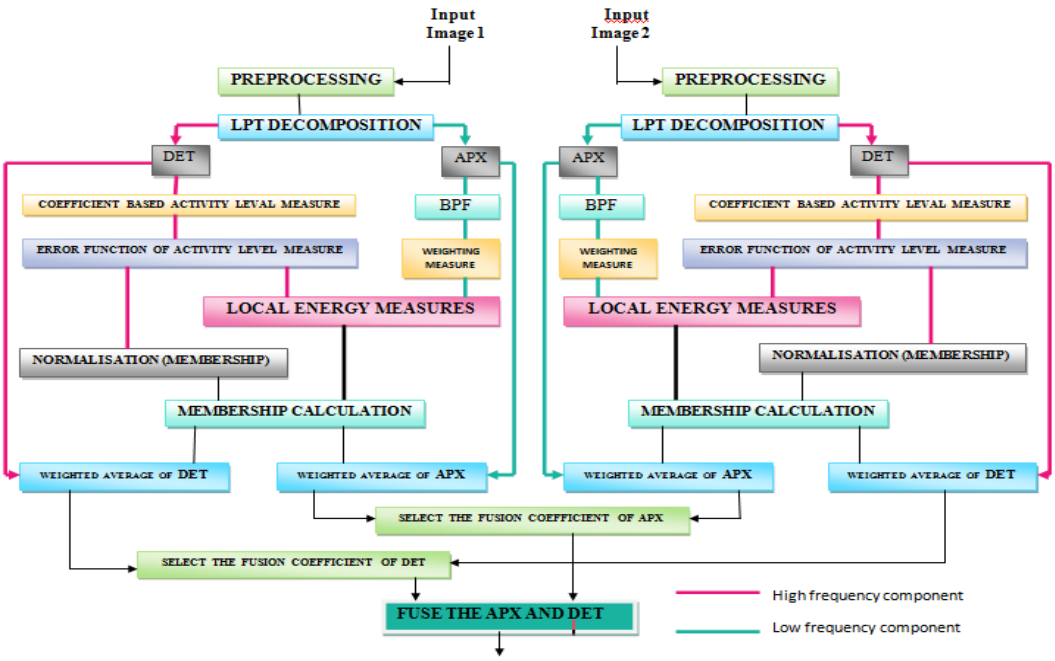

Figure 2. Flow Graph for Proposed Method

2. Flow Graph of NPS Fusion Rule

This flow graph shows that the different input images are fused after several steps , these steps are explained in section 3. The source images are assumed to be spatially registered, which is a common assumption in image fusion [1]. Various techniques can be applied to medical image registration. We follow the MSD-based fusion procedure, as illustrated in Figure 2.

3. Problem Formulation

Let $x^n_{k,d,i}$ and $\bar{x}^n_{d,i}$ denote the ith coefficients in the dth subband at the nth DET of the MSR of the kth source image and the fused image, respectively, where $n \in [1, N]$. Let $y_{k,d,i}$ and $\bar{y}_{d,i}$denote the ith coefficients in the dth subband at the APX of the MSR of the kth source image and the fused image, respectively. We assume that a subband at the APX has the same size as a subband at the Nth DET. For PT schemes where the APX is at a higher level, applying an extra step of bandpass filtering can fulfill this assumption. Let $M : \{\bar{x}^n_{d,i}, \bar{y}_{d,i}\} \times \{x^n_{k,d,i}, y_{k,d,i}\} \to [0, 1]$ be a function representing the (partial) membership of $\bar{x}^n_{d,i}$ (or $\bar{y}_{d,i}$) to the MSR of the kth source image, *i.e.*, the proportion of the contribution from $x^n_{k,d,i}$ (or $y_{k,d,i}$) to $\bar{x}^n_{d,i}$ (or $\bar{y}_{d,i}$) among all corresponding coefficients $\{x^n_{k,d,i}\ |k = 1, \ldots, K\}$ $k = 1, \ldots, K\}$). The memberships can be determined based on local and/or global information in the MSRs. To simplify notation, let $M^n_{k,d,i}$ and $M_{k,d,i}$ denote the coefficient memberships at the nth DET and the APX, respectively. All the membership function range in the kth level is [0,1].

For each subband of a DET, where the corresponding coefficients among different MSRs are usually quite distinct from each other, a fused coefficient can be determined as the one with the highest membership:

$$\bar{x}^n_{d,i} = \arg\max_{x^n_{k,d,i}}, k: 1,2..k\ M^n_{k,d,i} \tag{1}$$

For the APX, where the corresponding coefficients usually exhibit less diversity compared to those at a DET, a fused coefficient can be determined as a weighted average of all of its corresponding coefficients based on their memberships:

$$\bar{y}_{d,i} = \sum_{k=1}^{k} M_{k,d,i} y_{k,d,i} \tag{2}$$

4. Neighbouring Coefficient Selection

The proposed NPS fusion rule aims to pass information within and between each decomposition level to achieve intrascale and interscale consistencies so that the fused image preserves the most details from the source images while exhibiting minimal artifacts. The basic steps are: 1) pass salient information from a lower level to a higher level in an MSR until APX is reached; 2) calculate the memberships of each fused coefficient at APX using the passed salient information; 3) use these memberships to guide the coefficient selection at DETs.

Let $X^n{}_{k,d,i}$ denote the activity level of $x^n{}_{k,d,i}$. In order to impose interscale consistency, the activity levels of coefficients at a lower decomposition level are passed to a higher level as follows:

$$\bar{X}^n_{k,d,i} = \begin{cases} \operatorname{erf}\left(X^n_{k,d,i}\right), & n = 1 \\ \max\left(\operatorname{erf}\left(X^n_{k,d,i}\right), \left[\bar{X}^{n-1}_{k,d,i}\right]^{\downarrow 2}\right), & n \in [2, N] \end{cases} \tag{3}$$

where $\bar{X}^n_{k,d,}$ denotes the vector containing all, $\bar{X}^n_{k,d,i}$,is in the dth subband of the MSR of the kth source image; $[\cdot]\downarrow 2$ denote downsampling by a factor of 2 in each dimension; and the subscript$[\cdot]i$ denotes the ith coefficient. The maximum function is used as a way to ensure interscale consistency by allowing the calculation at higher scales to access the most representative salient information at lower scales, which we take as those with high activity levels. erf : R → [−1, 1] is called the Gauss error function, a sigmoid-shaped function. The magnitudes of activity levels of coefficients across different DETs can vary significantly, which makes it difficult to compare the relative importance of salient information across scales. This nonlinear function erf(·) compresses the activity levels into the same range [0, 1] for non-negative activity levels, which gives a more reasonable comparison of salient information. In addition, it also depresses very high activity levels, which sometimes may be caused by image noise.

At the APX, the passed salient information , $\bar{X}^N_{k,d,i}$is and the approximation coefficients $y_{k,d,i}$ is are used together to calculate the memberships $M_{k,d,i}$ s. One simple scheme is to directly take normalized $\bar{X}^N_{k,d,i}$,is as $M_{k,d,i}$ s. However, this scheme does not utilize the visual information embedded in $y_{k,d,i}$s, which is crucial for producing locally smoothed solutions. The generalized random walks (GRW) proposed in has demonstrated good performance in imposing intrascale consistency, while preserving local details in multi exposure fusion. Therefore, here we employ GRW to calculate $M_{k,d,i}$ s, which we consider as the steady-state probabilities in the random walks context, by minimizing K similarly defined energy functions. Let $M_{k,d}$ denote the vector containing all $M_{k,d,i}$s, *i.e.*, memberships of all the approximation coefficients in the dth subband of the fused MSR to the kth source image. The solution to the kth energy function is given by

$$L_d M_{k,d} = \bar{X}^N_{k,d} \tag{4}$$

The matrix L_d encodes the similarities between adjacent coefficients. The entry in the ith row and jth column of L_d is defined as follows:

$$L_{d,i,j} = \begin{cases} \sum_{\bar{y}_{d,i} \in N_{d'}} S_{d,i} + \sum_k \bar{X}^N_{k,d}, & i = j \\ -W_{d,i,j} & \bar{y}_{d,i} \in N_{d,i} \\ o, & otherwise \end{cases} \tag{5}$$

where $N_{d,i}$ is the first-order neighborhood of $\bar{y}_{d,i}$. $S_{d,i,j}$ represents the expected similarity between $\bar{y}_{d,i}$ and $\bar{y}_{d,j}$ based on the observed approximation coefficients in the MSRs of the source images. $S_{d,i,j}$ is defined as follows:

$$S_{d,i,j} = \gamma \prod_{k=1}^{k} \exp\left(-\frac{\|y_{k,d,i} - y_{k,d,j}\|}{\sigma}\right) \tag{6}$$

where γ and σ are weighting factors. Equation (6) assigns a higher penalty to a coefficient pair with greater similarity. Therefore, similar coefficients are more likely to be assigned similar memberships to ensure intrascale consistency. Once $M_{k,d}$,is calculated for the APX (n = N) using (4) to (6), they are passed down to guide the membership calculation at DETs to impose interscale consistency

$$M_{k,d,i}^{n} = \begin{cases} M_{k,d,i} & n = N \\ \frac{1}{\alpha}\left(\left[\emptyset * \left(\bar{X}_{k,d}^{n} \blacksquare \left[M_{k,d}^{n+1}\right]^{\uparrow 2}\right)\right]\right), & n \in [1, N-1] \end{cases} \tag{7}$$

where α is a normalization factor rendering $M_{k,d,i}^{n}$= 1; [·]↑2 denotes up sampling by a factor of 2 in each dimension followed by interpolation; $*$ denotes convolution; _ denotes component-wise multiplication; and φ is a low-pass filter that helps to achieve intrascale consistency. In our current implementation, φ is taken as a 5 × 5 × 5 Gaussian filter for each decomposition level of a volume.

5. LPT+NPS Based Fusion

In order to combine our NPS rule with LPT, an extra step of bandpass filtering at the APX is needed to produce a corresponding DET. This DET is only used in the coefficient membership calculation and is not involved in IMSD. Please note that there is only one subband at each decomposition level for LPT. The whole process of LPT+NPS based fusion is summarized in Algorithm.

6. NPS Fusion Algorithm

1. Apply LPT to source images for decomposition
2. Apply BPF to APX components of input images.
3. Compute activity level of DET component.
4. Compute membership calculation to APX and DET
5. Select the coefficient for fused DET and APX
6. Apply inverse LPT to fused coefficients.

IV. Evaluation Criteria

The performance of our NPS fusion rule was evaluated on 2D image fusion of CT and MRI scan images After this validation, we demonstrate the capability of our fusion rule to fuse other modalities (see Section V). In addition, we have consulted a neurosurgeon and a radiologist. In their opinion, our method not only provides enhanced representations of information, which is useful in applications like diagnosis and neuronavigation, but also offers them the flexibility of combining modalities of their choice, which is important because the data types required are normally application dependent.

Objective image quality measures play an important role in various image processing applications. There are different types of object quality or distortion assessment approaches. The fused images are evaluated, taking the following parameters into consideration.

1. Root Mean Square error (RMSE)

The root mean square error (RMSE) between each unsharpened MS band and corresponding sharpened band can also be computed as a measure of spectral fidelity. It measures the amount of change per pixel due to the processing.

The RMSE between a reference image R and the fused image F is given by

$$E1 = \sqrt{\frac{1}{MN}\sum_{i=1}^{M}\sum\nolimits_{j=1}^{N}\left(R(i,j) - F(i,j)\right)^2} \tag{8}$$

There are different approaches to construct reference image using input images. In our experiments, we used the following procedure to compute RMSE.

First, RMSE value El is computed between source image A and fused image F.

$$E1 = \sqrt{\frac{1}{MN}\sum_{i=1}^{M}\sum\nolimits_{j=1}^{N}\left(I1(i,j) - F(i,j)\right)^2} \tag{9}$$

Similarly E2 is computed as RMSE between source image B and fused image F.

$$E2 = \sqrt{\frac{1}{MN}\sum_{i=1}^{M}\sum\nolimits_{j=1}^{N}\left(I2(i,j) - F(i,j)\right)^2} \tag{10}$$

Then the overall RMSE value is obtained by taking the average of E1 and E2.

$$RMSE = \frac{(E1+E2)}{2} \tag{11}$$

Smaller RMSE value indicates good fusion quality.

2. Peak Signal to Noise Ratio

PSNR can be calculated by using the formula

$$\text{PSNR} = 20\log_{10}[\frac{L^2}{MSE}] \tag{12}$$

3. Image Quality Index

IQI measures the similarity between two images (I1 & I2) and its value ranges from -1 to 1. IQI is equal to 1 if both images are identical. IQI measure is given by

$$IQI = \frac{m_{ab}}{m_a m_b}\frac{2xy}{x^2+y^2}\frac{2m_a m_b}{m_a^2+m_b^2} \tag{13}$$

Where x and y denote the mean values of images I1 and I2 and m_a^2, m_b^2, and m_{ab} denotes the variance of I1 , I2 and covariance of I1 and I2.

4. Mutual Information

Mutual Information (MI) measures the degree of dependence of two images. Its value is zero when I1 and I2 are independent of each other. MI between two source images I1 and I2 and fused image F is given by

$$MI = \sum_{(f,a)} P_{FA}(f,a) \log_2 \frac{P_{FA}(f,a)}{P_F(f)P_A(a)} + \sum_{(f,b)} P_{FB}(f,b) \log_2 \frac{P_{FA}(f,b)}{P_F(f)P_b(b)} \quad (14)$$

and $P_A(a)$,$P_B(b)$ and $P_F(f)$ are histograms of images A, B and F,$P_{FA}(f,a)$ *and* $P_{FB}(f,b)$ are the joint histograms of F and A, and F and B respectively. Higher MI value indicates good fusion results.

5. Objective Evaluation Metric

The objective metric $Q^{AB/F}$ [14] was employed in evaluating the fusion quality. This metric does not require an ideal composite image, which is difficult to get in practical cases, as a reference image. $Q^{AB/F}$ has been proven to correspond well with subjective tests among different metrics and is widely used to assess fusion quality. $Q^{AB/F}$ measures the amount of edge information correctly transferred from source images to the fused image; a $Q^{AB/F}$ score is within the range [0, 1], where a higher score indicates a better fusion result.

V. Result Analysis

In this paper, we compared different sets of fusion rule with NPS fusion rule. We have taken different multi modality medical images such as MRI, PET, CT. The proposed method is compared with DWT. The DWT perform the operation up to the 2 level decomposition which gives the good fusion quality and reduces the artifact effect. When the image size is increased and the number of decomposition level also increases, it leads the artifact effect in fused image. LPT does not affect the quality of fused image, even we increase the decomposition level. It gives the better result for different size of input images 512*512, 256*256, 128*128. Table.1 shows the performance of the proposed image fusion method where the input images are MRI and PET images and the image size is 512*512. Table.2 shows the performance of MRI and CT images and the image size is 256*256.

Table 1. Performance Comparison of Proposed Method

Fusion Rule	NG+AVG+CM+NV		NG+AVG+CM+WBV		NG+WG+CM+WBV		NPS	
MSD Technique	DWT	LPT	DWT	LPT	DWT	LPT	DWT	LPT
$Q^{AB/F}$	0.5610	0.6566	0.6719	0.7022	0.5481	0.6529	0.7217	**0.7727**
MI	5.2340	5.3765	5.9867	6.1076	6.3490	6.6098	7.8760	**7.9078**
RMSE	11.876	12.123	12.895	13.109	14.897	15.678	16.567	**17.147**
PSNR	25.673	30.187	27.971	31.456	24.569	29.845	30.764	**32.678**

Table 2. Performance Comparison of Proposed Method

Fusion Rule	NG+AVG+CM+NV		NG+AVG+CM+WBV		NG+WG+CM+WBV		NPS	
MSD Technique	DWT	LPT	DWT	LPT	DWT	LPT	DWT	LPT
$Q^{AB/F}$	0.5201	0.5634	0.5921	0.6102	0.5061	0.6271	0.6541	**0.6790**
MI	5.1670	5.2184	5.7845	5.9161	6.1901	6.2567	6.6981	**6.8541**
RMSE	9.8931	10.743	11.287	12.365	13.654	14.724	15.764	**16.645**
PSNR	22.783	24.389	25.120	26.874	27.123	28.873	29.651	**30.719**

The various fusion rule sets perform the image fusion in different modalities of medical images. Our NPS rule produce the best performance in transferring edge information on both datasets, as indicated by the highest $Q^{AB/F}$ scores. LPT performs better than DWT for these datasets. When the other settings are the same, WBV performs better than NV and CBV, and AVG performs better than WA. Therefore, for brevity, only NG+AVG+CM+WBV, CBSG+AVG+CM+WBV, and MG+CM+CM+WBV are visually compared with our NPS rule on the lesion dataset in Figure 5.

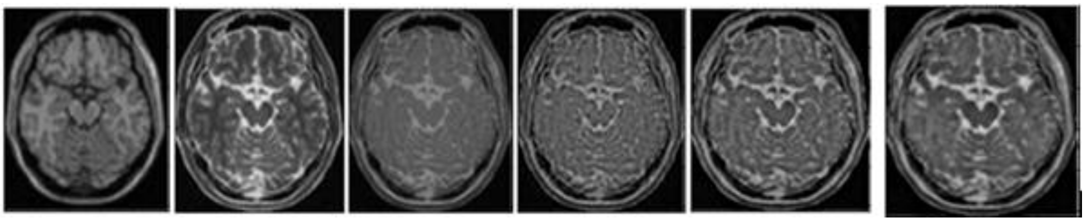

A B C D E F

Figure 3. Comparison of Different Fusion Rules. (a) CT Image, (b) MRI Image, (c) LPT+NG+AVG+CM+NV, (d)LPT+NG+AVG+CM+WBV, (e) LPT+NG+WG+CM+WBV, (f) LPT+ NPS

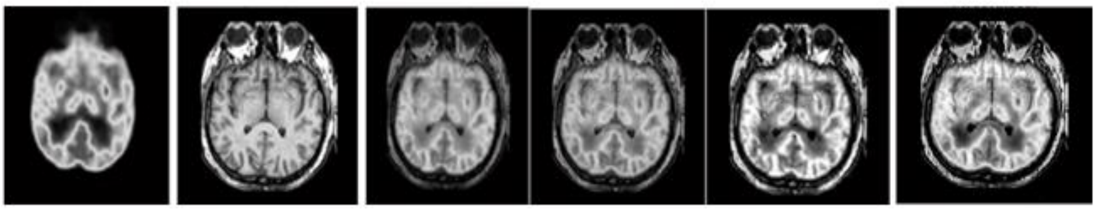

A B C D E F

Figure 4. Comparison of Different Fusion Rules. (a) PET Image, (b) MRI Image, (c) LPT+NG+AVG+CM+NV, (d)LPT+NG+AVG+CM+WBV, (e)LPT+NG+WG+CM+WBV, (f)LPT+ NPS

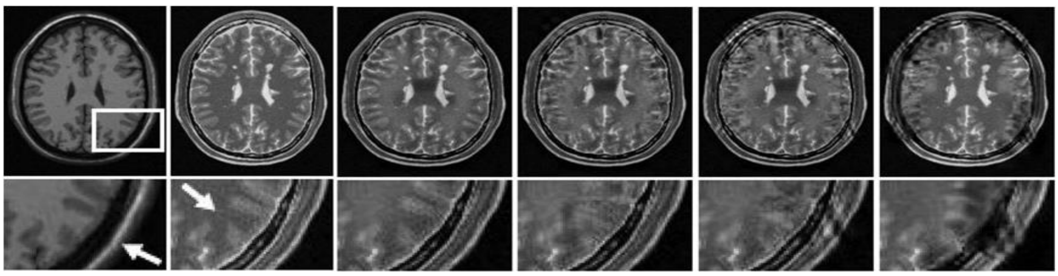

A B C D E F

Figure 5. Comparison of Different Fusion Rules. (a) CT Image, (b) MRI Image, (c) LPT+NG+AVG+CM+NV, (d) LPT+NG+AVG+CM+WBV, (e) LPT+NG+WG+CM+WBV, (f) LPT+NPS

The formulation of image fusion as membership calculation, together with the consistency constraints imposed in our NPS fusion rule, helps to ensure that associated coefficients are fused similarly in order to avoid fusion artifacts, and to ensure that salient information (*e.g.*, edge information) is correctly transferred from the source images to the fused image. Therefore, compared to other fusion rules, our NPS rule not only correctly combined information with high consistency with the source images, but also provided good local contrasts (*e.g.*, between ventricles, gray matter and white matter). As shown in the insets below each slice, our NPS rule successfully eliminated the blocking artifacts shown in MG when coupled with LPT, and it eliminated the aliasing artifacts in NG, CBSG, and MG when coupled with DWT.

VI. Conclusion

In this proposed work, Neighbouring Pixel Coefficient Selection fusion rules are implemented for each decomposition level, an optimal set of coefficients are selected. In practice higher quality images are obtained in the image fusion. Using monochrome fusion, results are demonstrated. In addition to this many extra features can be implemented such as avoid fusion artifacts, provided good local contrasts, maintain intra and inter scale consistency by extending our techniques and also performing for individual applications by this technique.

References

[1] R. S. Blum, Z. Xue and Z. Zhang, “An overview of image fusion”, in Multi-Sensor Image Fusion and Its Applications. Boca Raton, FL: CRC Press, **(2005)**, pp. 1–36.
[2] M. I. Smith and J. P. Heather, “A review of image fusion technology in 2005”, Proc. SPIE, vol. 5782, **(2005)**, pp. 29–45.
[3] G. Piella, “A general framework for multiresolution image fusion: from pixels to regions”, Inf. Fusion, vol. 4, no. 4, **(2003)**, pp. 259–280.
[4] S. Li, B. Yang and J. Hu, “Performance comparison of different multi-resolution transforms for image fusion”, Inf. Fusion, vol. 12, no. 2, **(2011)**, pp. 74–84.
[5] M. C. Valdes, Hernandez, K. Ferguson, F. Chappell and J. Wardlaw, “New multispectral MRI data fusion technique for white matter lesion segmentation: method and comparison with thresholding in FLAIR images”, Eur. Radiol., vol. 20, no. 7, **(2010)**, pp. 1684–1691.
[6] G. Pajares and J. M. de la Cruz, “A wavelet-based image fusion tutorial”, Pattern Recognition, vol. 37, no. 9, **(2004)**, pp. 1855–1872.
[7] H. Li, B. S. Manjunath and S. K. Mitra, “Multisensor image fusion using the wavelet transform,” Graph. Models Image Process, vol. 57, no. 3, **(1995)**, pp. 235–245.
[8] V. Petrovic´ and C. Xydeas, “Cross-band pixel selection in multiresolution image fusion”, Proc. SPIE, vol. 3719, **(1999)**, pp. 319–326.
[9] Z. Zhang and R. S. Blum, “Region-based image fusion scheme for con-cealed weapon detection”, Proc. Annu. Conf. Inf. Sci. Syst., **(1997)**, pp. 168–173.
[10] P. J. Burt and R. J. Kolczynski, “Enhanced image capture through fusion”, Proc. Int. Conf. Comput. Vis., **(1993)**, pp. 173–182.
[11] K. Rajpoot, J. A. Noble, V. Grau, C. Szmigielski and H. Becher, “Multi-view RT3D echocardiography image fusion”, Proc. FIMH, vol. 5528, **(2009)**, pp. 134–143.
[12] Z. Wang and Y. Ma, “Medical image fusion using m-PCNN”, Inf. Fusion, vol. 9, no. 2, **(2008)**, pp. 176-485.
[13] Y. Yang, D. S. Park, S. Huang and N. Rao, “Medical image fusion via an effective wavelet-based approach,” EURASIP J. Adv. Signal Process., vol. 2010, no. 579341, **(2010)**, pp. 1–13.
[14] A. Toet, “Natural colour mapping for multiband nightvision imagery”, Inf. Fusion, vol. 4, no. 3, **(2003)**.
[15] J. M. Rovamo, M. I. Kankaanpaa and H. Kukkonen, “Modelling spatial contrast sensitivity functions for chromatic and luminance-modulated gratings”, vol. 39, no. 14, **(1999)**, pp. 2387–2398.

Authors

Sivasangumani. S, Obtained his Bachelor of Engineering degree in Electronics and Communication Engineering from V.S.B Engineering College Affiliated to Anna University, Karur, Tamil Nadu, India. in 2012. He is currently doing his Master of Engineering in Applied Electronics in V.S.B Engineering College, Affiliated to Anna University, Karur, Tamil Nadu, India. He has published three papers in different International journal and also he has presented six papers in different National, International Conference. His areas of interest include Image Processing, Fuzzy Logic, Pulse Coupled Neural Networks and Digital Electronics.

P. S. Gomathi, received B.E degree in Electrical and Electronics Engineering and M.E degree from Bharathiar University, India in 1998, 2000 respectively. Currently, she is working as an Assistant Professor in the Department of Electronics and Communication Engineering, V.S.B. Engineering College, Karur. Her research interest includes Digital Image Processing, Neural Networks and Fuzzy logic. Her publication includes several papers in National /International conferences and journals.

B. Kalaavathi, received B.E. Degree in Computer Science Engineering from Bharathiar University,India in 1993 and M.Tech from Pondicherry University, India in 2000. She received Ph.D degree from Periyar University, India in 2010. Currently, she is working as a Professor in Department of Computer Science and Engineering, K.S.R Institute for Engineering and Technology, Tiruchengode. Her research areas of interest include Digital Image Processing and Mobile Computing. She has over 16 years of Experience in teaching. Her publication includes 7 journal papers and 10 National /International Conferences.